

# Fatigue behavior of silica fibers with different defects

Sergei L. Semjonov<sup>a\*</sup>, G. Scott Glaesemann<sup>b</sup>, Donald A. Clark<sup>b</sup> and Mikhail M. Bubnov<sup>a</sup>

<sup>a</sup>Fiber Optics Research Center, Moscow, Russia

<sup>b</sup>Corning Inc., Corning, NY

## ABSTRACT

Comparison of high-speed strength data for weak (abraded, contaminated and indented) and pristine fibers was performed. It was shown that fatigue behavior of abraded fiber practically coincides with that of the fiber contaminated by zirconia powder and is close to that of indented fiber. The fatigue parameters obtained for strong pristine fiber cannot be used to obtain the correct prediction of fiber strength after proof testing. A two-region power law model was used for mathematical description of these results and the fatigue parameters for three types of weak fibers were obtained.

## 1. INTRODUCTION

Lifetime modeling of optical fiber is often based on the results and parameters obtained from strong, “flaw-free” fibers. The fatigue parameter  $n \sim 20$  is used for both calculation of the fiber strength after proof testing as well as the evaluation of strength degradation during the in-service lifetime. However, the reliability of optical fibers in most communication systems depends on large ( $\sim 1 \mu\text{m}$ ) flaws, which can survive proof testing at  $\sim 0.7 \text{ GPa}$ . Only a few flaws of this kind exist on multi-kilometer fiber lengths. In order to study the fatigue of such flaws, weak fibers with narrow strength distributions over short lengths must be specially prepared. Early research on such flaws in fiber were conducted using relatively simple fatigue tests over a narrow range of loading speeds and a fatigue parameter  $n \sim 20$  was typically measured.<sup>1-4</sup> The latest reports from dynamic fatigue measurements conducted over a wide range of stressing rates demonstrate a complicated multi-region fatigue behavior at high stressing rates for abraded and indented fibers.<sup>5-7</sup> Owing to crack growth during the proof testing,<sup>8,9</sup> evaluation of the fiber strength after proof testing is very sensitive to the fatigue behavior observed at high stressing rates.<sup>5</sup> Thus, a detailed study of the fatigue behavior of weak fibers in as wide a range of stressing rate as possible is required for adequate lifetime modeling. Moreover, a comparison of the fatigue behavior of different types of possible defects (indented, abraded, and contaminated) should help in understanding the real contribution of both the initial defect shape and possible localized residual stresses. Additionally, initial or liquid nitrogen strength of these flaw types should be measured to further quantify the fatigue behavior.<sup>10</sup>

This paper continues the study of the properties of weak fibers, that was started with high-speed testing of abraded<sup>5,11</sup> and indented<sup>7</sup> fibers. New samples of weak fibers with melted-in zirconia particles have been fabricated and tested. A method of measuring the liquid nitrogen strength for continuously damaged fibers has been developed. Using the initial strength data, results for indented, abraded and contaminated samples are compared, and fatigue parameters for such fibers are calculated.

## 2. EXPERIMENTAL PROCEDURE

A special apparatus for tensile testing weak fibers over a wide region of stressing rates was already described in detail earlier.<sup>5,11</sup> In this study, 10 cm coated fiber samples were tensile tested. To avoid premature failure where the fiber is gripped, weak fiber ends were glued to pieces of strong fibers by epoxy. Only failures in the gauge length were accepted. 25 samples were usually tested at each stressing rate.

Measurements at liquid nitrogen temperature were performed using a small horizontal thermoisolated bath with narrow slots for introducing the fiber sample. The fiber's acrylate coating and the epoxy glue become very hard and brittle at such low temperatures. Thus, the polymer coating was removed by hot sulfuric acid from samples to be tested at liquid nitrogen temperature and a silicone rubber sealant was used instead of epoxy glue. Too soft for testing at room temperature, this

---

\* Correspondence: E-mail: sls@fo.gpi.ru; Telephone: 7(095)135-7402; Fax: 7(095)135-8139

sealant became hard but not brittle in liquid nitrogen. As with the fatigue testing, only failures in the gauge length were accepted.

Weak fibers were created by drawing fiber whose surface had been seeded with zirconia powder (~ 1 μm particle size) while still in the preform stage. The particles were melted into the preform surface prior to draw. To make the distribution of particles on the preform surface more homogenous, the preform was washed in an alcohol solution containing the zirconia powder. The density of particles in the solution was systematically changed to optimize the strength distribution for 10cm long samples. A Weibull modulus, m, of approximately 20 was obtained. The strength distributions for each stressing rate are shown in Figure 1. This rather narrow strength distribution enabled us to accurately view the strength variation with stressing rate.

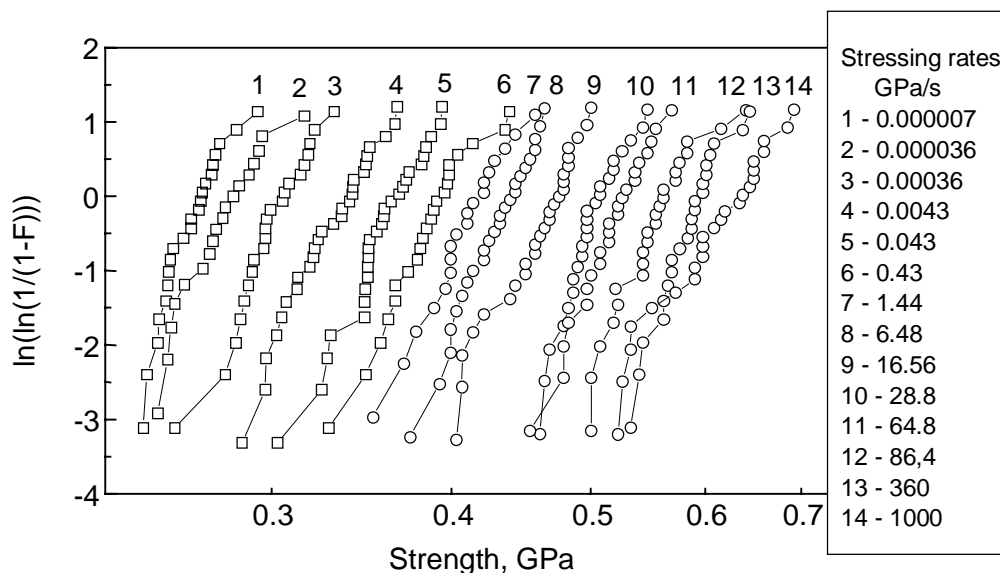


Figure 1. Zirconia-seeded fiber strength measured at different stressing rates in a laboratory environment.

For comparison purposes, another fiber was abraded by a silica rod situated above the polymer applicator during the drawing process. This abrasion process was also optimized to yield a Weibull modulus of 20 on 10-cm long samples. These abraded samples were tested under the same conditions (50% RH, 23°C and in liquid nitrogen) as the zirconia seeded fibers.

### 3. RESULTS AND ANALYSIS

Plots of the median strength of seeded and abraded samples tested in a laboratory environment (50% RH, 23°C) are given in Figure 2. Both plots demonstrate a nonlinear strength versus stressing rate behavior when plotted in the usual power-law fashion. A direct comparison of the fatigue behavior of the two fibers in Figure 2 is hampered by the difference in initial strength between the two fibers. It has been shown in a previous paper<sup>10</sup> that  $(\sigma_d / S_i) - (\sigma' / S_i^3)$  are universal coordinates for presentation of dynamic fatigue data. Here  $\sigma_d$  is the median strength of a fiber at stressing rate  $\sigma'$ , and  $S_i$  is the initial (inert) strength of the same fiber. Usage of these coordinates helps to compare fatigue data regardless of the initial defect size. The strength in liquid nitrogen (Figure 3) was used for the determination  $S_i$ . The dynamic fatigue data for seeded and abraded fibers is shown in universal coordinates in Figure 4. Both fibers exhibit very similar non-linear fatigue behavior despite the difference in flaw type and initial strength. It has been hypothesized that this non-linear fatigue behavior can be attributed to the influence of region II crack growth at high speeds or short times to failure.<sup>5</sup> The mathematical description of this behavior is the joining of two power law equations:

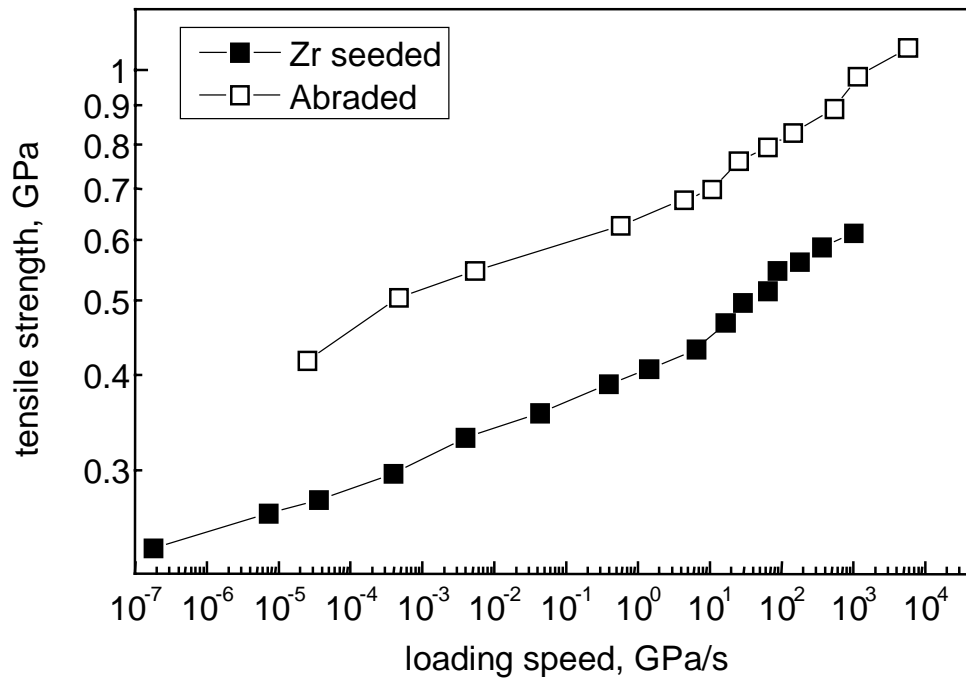


Figure 2. Median strength of seeded and abraded samples tested in laboratory environment (50% RH, 23°C)

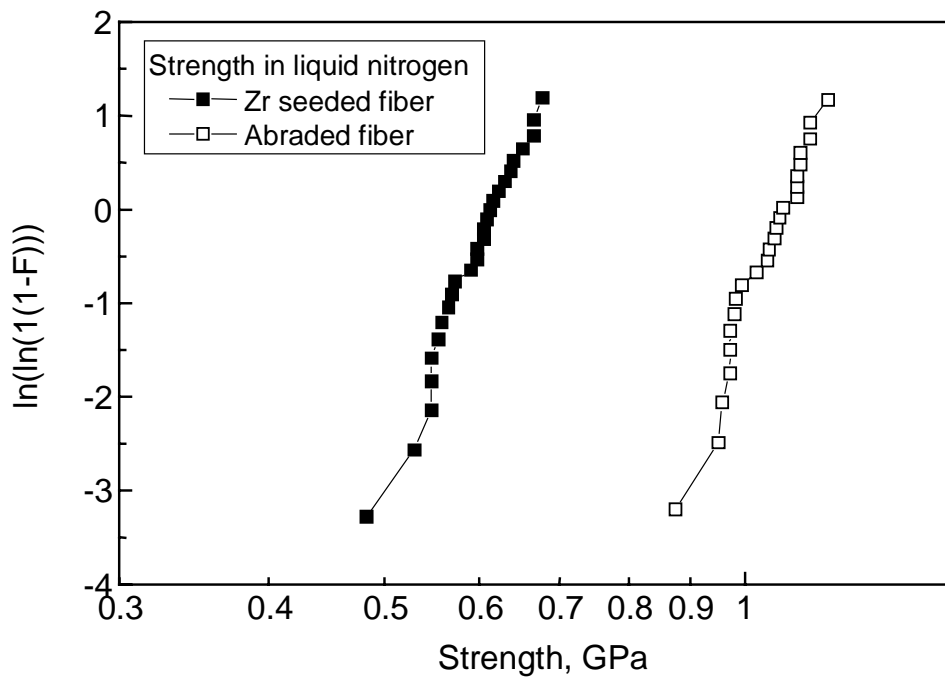


Figure 3. Strength of zirconia-seeded fiber and abraded fiber measured in liquid nitrogen.

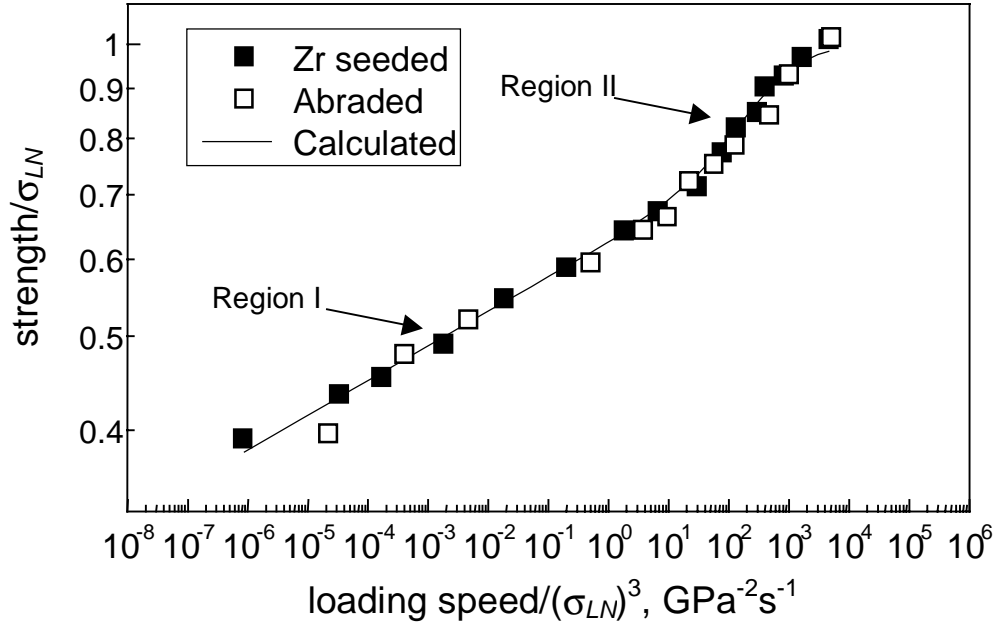


Figure 4. Median strength of seeded and abraded samples tested in laboratory environment (50% RH, 23°C) plotted in “universal” coordinates.

$$\frac{da}{dt} = v_1 \left( \frac{K_I}{K_{IC}} \right)^{n_1} \quad \text{for } K_I \leq r K_{IC} \quad (1)$$

$$\frac{da}{dt} = v_2 \left( \frac{K_I}{K_{IC}} \right)^{n_2} \quad \text{for } K_I \geq r K_{IC} \quad (2)$$

where  $K_I$  is the stress intensity factor,  $K_{IC}$  is the critical stress intensity factor associated with failure,  $da/dt$  is the flaw growth rate,  $v_1$ ,  $v_2$ ,  $n_1$  and  $n_2$  are the parameters of the respective curves. The parameter  $r$  and the relation  $v_1 = v_2 \cdot r^{(n_2-n_1)}$  characterize the point of transition of flaw growth rate from Region I to Region II.

These equations can be rewritten for the case of dynamic fatigue tests in terms of the changing inert strength,  $S$ , and applied stress  $\sigma$ , using usual relations,  $K_I = Y \sigma a^{1/2}$  and  $K_{IC} = Y S a^{1/2}$ , where  $Y$  is the geometric factor of the flaw:

$$S_i^{n_1-2} = S_r^{n_1-2} + \frac{\sigma_r^{n_1+1}}{B_1(n_1+1)\sigma'} \quad \text{for flaw growth through Region I} \quad (3)$$

$$S_r^{n_2-2} = \sigma_d^{n_2-2} + \frac{\sigma_d^{n_2+1} - \sigma_r^{n_2+1}}{B_2(n_2+1)\sigma'} \quad \text{for flaw growth through Region II} \quad (4)$$

where  $S_i$  is the initial strength before loading,  $S_r$  and  $\sigma_r$  are the inert strength and applied stress when  $K_I/K_{IC} = \sigma_r/S_r = r$ ,  $\sigma_d$  is the dynamic fatigue strength for stress rate  $\sigma'$ ,  $1/B_2 = v_2(Y/K_{IC})^2(n_2-2)/2$  and  $B_1 = B_2 \cdot r^{(n_1-n_2)}(n_2-2)/(n_1-2)$ .

The following substitution

$$\begin{cases} x = \sigma' / S_i^3 \\ y = S / S_i \end{cases} \quad (5)$$

enables us to transform Equations (3) and (4) into a system of equations:

$$\begin{cases} 1 = y_r^{n_1-2} + \frac{r^{n_1+1} y_r^{n_1+1}}{B_1(n_1+1)x} \\ y_r^{n_2-2} = y_d^{n_2-2} + \frac{y_d^{n_2+1} - r^{n_2+1} y_r^{n_2+1}}{B_2(n_2+1)x} \end{cases} \quad \text{where } y_d < y_r < 1 \quad (6)$$

Solution of this system  $y_d(x) = \sigma_d / S_i(\sigma' / S_i^3)$  describes the dynamic fatigue behavior of the fiber in the universal coordinates. Unfortunately, there is no exact analytical solution for this function. Thus, numerical simulation of this function with variation of all the fatigue parameters was performed to achieve the best fit to experimental data.

The result of this simulation for both seeded and abraded fibers is given in Figure 3 as solid line. The corresponding fatigue parameters are shown in Table 1.

Table 1. Fatigue parameters for seeded and abraded fibers

$n_1$	27
$B_1$	$0.7 \times 10^{-7} \text{ GPa}^2\text{s}$
$r$	0.757
$n_2$	0.5
$B_2$	$-1.9 \times 10^{-3} \text{ GPa}^2\text{s}^*$

#### 4. DISCUSSION

The results of testing abraded and contaminated fibers are compared with the results for indented and pristine fibers obtained in earlier studies<sup>7,10</sup> in Figure 5. Unfortunately, measuring the liquid nitrogen strength of strong pristine fiber was problematic owing to problems with the glue. Thus, previously published values of 12 GPa and 14 GPa were used.<sup>12,13</sup>

Comparison with high strength fiber is limited due to testing difficulties of pristine fibers at high speeds, but at slower speeds there is a clear discrepancy between high strength and low strength results. Numerical approximation gives fatigue parameters for the indented and pristine fibers shown in Table 2.

Table 2. Fatigue parameters for indented and pristine fibers

Parameter	Indented fiber	Pristine fiber
$n_1$	31	20
$B_1$	$0.4 \times 10^{-9} \text{ GPa}^2\text{s}$	$3.1 \times 10^{-6} \text{ GPa}^2\text{s}$ ( $S_i = 12 \text{ GPa}$ ) $1.6 \times 10^{-7} \text{ GPa}^2\text{s}$ ( $S_i = 14 \text{ GPa}$ )
$r$	0.70	not available
$n_2$	3.0	not available
$B_2$	$2.5 \times 10^{-4} \text{ GPa}^2\text{s}$	not available

The shape of the fatigue curve generated by the indented samples in Figure 5 is close to that of the abraded and contaminated fibers. This suggests that fatigue of flaws in silica is independent of the flaw introduction mechanism and that the form of the crack velocity function for surface flaws in silica-clad optical fiber is independent of flaw type. This is important since it simplifies reliability modeling of the multiple flaw populations known to exist in optical fiber. One does not have to have a separate model for each flaw type.

\*  $B_2$ -value is negative because  $n_2 < 2$ .

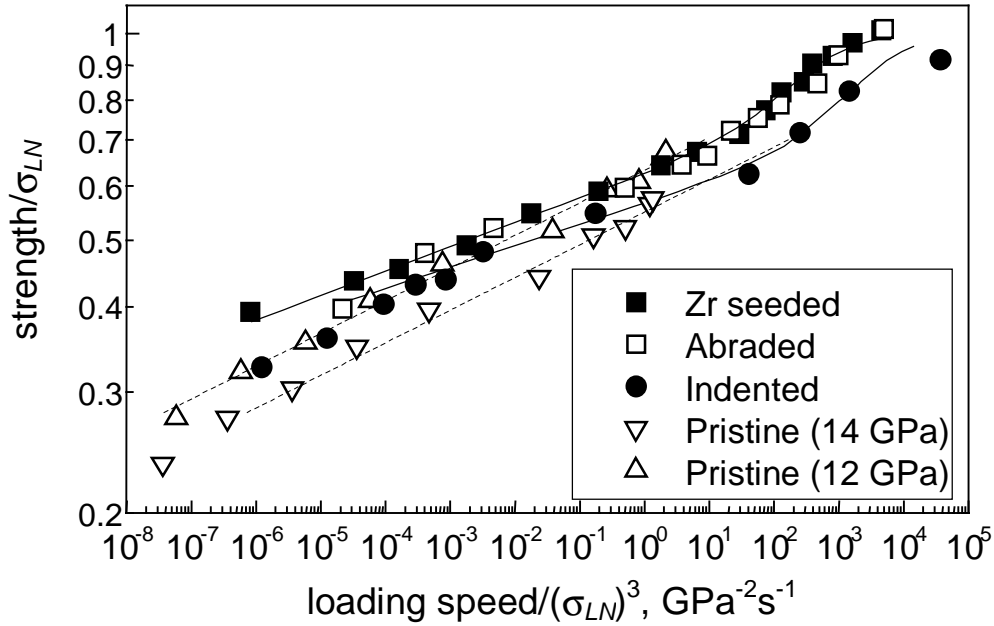


Figure 5. Joint plot of dynamic fatigue results obtained for different types of weak fibers and pristine fiber.

In universal coordinates the indented strength is somewhat lower than that of the contaminated and abraded specimens. There are several possible factors that could contribute to this difference. The three factors discussed here represent areas of further investigation. First, the role of the contact-induced residual stress of the indented specimens was not taken into account in determining the failure stress. The residual stress is known to promote subcritical crack growth in fatigue environments, and therefore, yield a lower fatigue strength. The mechanics have been developed for such determinations,<sup>14,15,16</sup> but accurate quantification of residual stress levels is lacking. It should be noted that the partially submerged zirconia particles on the contaminated fiber create significant residual stresses in the host silica.<sup>17</sup> The residual stress associated with zirconia particulate dissipates much quicker than that associated with indents as one moves away from the flaw tip. Crack growth mechanics that incorporates the influence of residual stresses associated with contaminants has yet to be developed. Note that the flaws associated with the sliding contact of draw-abrasion lack any appreciable contact residual stress. The second explanation for the lower universal fatigue strength for the indented specimens is crack geometry. An indirect method for assessing the role crack geometry would be to perform the same tests using cube corner indents.<sup>7</sup> The flaws associated with cube corner indentation are on the order of 1  $\mu\text{m}$  in size with virtually no residual stress. Thirdly, the indented specimens are not covered with polymer coating. The local environment for the coated flaws would certainly be different than that of uncoated flaws. Even if the local environment of a coated flaw were known, the influence of this environment on crack growth kinetics is unresolved. An experimental approach would at least yield empirical understanding of the coating influence for the data presented here.

Abrasions and melted-in particles are the most common flaws on the fiber surface. Proof testing of these flaws is usually performed under ambient conditions and so the fatigue parameters obtained for abraded and contaminated fibers at 50%RH and 23°C can be directly used for prediction of the inert strength after proof testing and, importantly, the minimum surviving strength. Owing to the growth of flaws under stress during proof testing the minimum surviving strength can be close to the proof test stress,  $\sigma_p$ , or be significantly less than that level depending on whether unloading is “fast” or “slow”<sup>5,9</sup>. The requirement for the case of “fast” unloading is simply:<sup>9</sup>

$$t_u < t_c = \frac{(n_2 - 2) \cdot B_2}{\sigma_p^2}, \quad (7)$$

where  $t_u$  is the time of unloading. Using the parameters obtained for abraded and contaminated fibers and  $\sigma_p = 0.7 \text{ GPa}$ , one obtains  $t_c = 5.8 \times 10^{-3} \text{ s}$ . The same parameter for indented fiber is  $0.51 \times 10^{-3} \text{ s}$ . These values are more achievable than the

$0.58 \times 10^{-5}$  s calculated in the case of single-region model and fatigue parameters obtained for strong fiber. Based on the results and analyses of this study the actual minimum surviving strength after proof testing is closer to the proof stress level than what one would predict using the single region power law and data obtained from high strength fiber.

This study was primarily focused on the behavior of weak fibers in the high stressing rates region. It should be emphasized that parameters of "Region I" obtained in this work cannot be simply used for the next step; namely, prediction of the long-term degradation of the fiber strength at low static stress during service. There are several papers where the fatigue parameter  $n$  is reported to be about 20 for the weak fibers in the region of slow stressing rates or at long-term static fatigue tests<sup>1-4,7,10</sup>. The most common explanation of  $n$ -value reduction at lower stressing rates is that the flaw growth should be described not by power function but by an exponential one.<sup>18</sup> In this case, parameter  $n_1$  is not a constant. Its value is expected to decrease with decreasing stressing rate.<sup>19</sup> However, there is little experimental evidence to support a decreasing  $n$  value over time for flaws near the proof stress level. From a field performance point of view, optical fiber design rules derived from the power law ( $\sigma_a = 1/5 \sigma_p$ ) have been robust in that few, if any, field failure can be attributed to the fatigue of flaws passing the proof stress. For improved lifetime predictions, the behavior of weak fibers at low stressing rates and low static loads should be investigated. This necessitates the use of abraded fiber with an extremely high Weibull modulus,  $m$ . In contrast with high-speed testing, it is important to perform such an investigation in various environments for simulating in-service conditions. Influence of polymer coating, defect shape and residual stresses will continue to be key factors. A question about possible crack pop-in effect due to residual stresses is also open. In the meantime, it is recommended that an  $n$  value of 20 be used for proof test level flaws placed in long-term service.

## 5. CONCLUSION

Comparison of high-speed testing data for weak (abraded, contaminated and indented) and pristine fibers was performed. It was found that fatigue behavior of abraded fiber practically coincides with that of the fiber contaminated by zirconia powder and is close to that of indented fiber. This suggests that the fatigue behavior of flaws in optical fiber is relatively independent of origin. Based on this and previous studies, the fatigue parameters obtained for strong pristine fiber using the single-region power law should not be used for modeling proof testing. A two-region power law model was used for mathematical description of the low strength flaws. The resulting fatigue parameters are believed to provide a more accurate prediction of post-proof strength needed in reliability predictions.

## 6. ACKNOWLEDGMENTS

Funding for this research was provided by Corning Incorporated.

## REFERENCES

1. S.P. Craig, W.J. Duncan, P.W. France and J.E. Snodgrass, "The strength and fatigue of large flaws in silica optical fibre," in *Proc. 8th ECOG* (Cannes, France), 1982.
2. F.A. Donaghy and D.R. Nicol, "Evaluation of the fatigue constant  $n$  in optical fibers with surface particle damage," *J. Amer. Ceram. Soc.*, **66** (8), pp. 601-604 (1983).
3. H.H. Yuce, P.L. Key and D.R. Biswas, "Investigation of the mechanical behavior of low strength fibers," in *Proc. SPIE*, **1174**, pp. 272-278 (1989).
4. G.S. Glaesemann, "The mechanical behavior of large flaws in optical fiber and their role in reliability predictions," *Int. Wire & Cable Symp. Proc.*, pp. 698-704 (1992).
5. T.A. Hanson, G.S. Glaesemann, "Incorporation multi-region crack growth into mechanical reliability predictions for optical fiber," *J. Materials Science*, **32**, pp. 5305-5311 (1997).
6. T. Volotinen, A. Breuls, N. Evanno et al., "Mechanical behavior and B-value of an abraded optical fiber," *47<sup>th</sup> Int. Wire & Cable Symp. Proc.*, pp. 881-890 (1998).
7. S.L. Semjonov, G.S. Glaesemann, C.R. Kurkjian and M.M. Bubnov, "Modeling of proof test level flaws using cube corner indents," *47<sup>th</sup> Int. Wire & Cable Symp. Proc.*, pp. 928-932 (1998).
8. A.G. Evans, S.M. Wiederhorn, "Proof testing of ceramic materials - an analytical basis for failure prediction," *Int. J. Fracture*, **10**, 379-392 (1974).
9. Y. Mitsunaga, Y. Katsuyama, H. Kobayashi, Y. Ishida, "Failure prediction for long length optical fiber based on proof testing," *J. Applied Phys.*, **53**(7), 4847-4853 (1982).

10. S.L. Semjonov, G.S. Glaesemann, and M.M. Bubnov, "Fatigue behavior of silica fibers of different strength," *Proc. SPIE*, **3848**, pp. 102-107 (1999).
11. G.S. Glaesemann, D.A. Clark, T.A. Hanson, D.J. Wissuchek, "High speed strength testing of optical fiber," *Mater. Research Soc. Symp. Proc.*, **531**, 249-260 (1998).
12. C.R. Kurkjian, D. Biswas and H.H. Yuce, "Intrinsic Strength of Lightguide Fibers," *Proc. SPIE*, **2611**, pp. 56-63 (1995).
13. B.A. Proctor, I Whitney, and J.W. Johnson, "The strength of fused silica," *Proc. Roy. Soc.* **297A**, 534 (1967).
14. S.R. Choi, J.E. Ritter, Jr., and K. Jackus, "Failure of Glass with Subthreshold Flaws," *J. Am. Ceram. Soc.*, **73**(2), 268-274 (1990).
15. D.H. Roach and A.R. Cooper, "Effect on Contact Residual Stress Relaxation on Fracture Strength of Indented Soda-Lime Glass," *J. Am. Ceram. Soc.*, **68** (11), 632-636 (1985).
16. T.P. Dabbs and B.R. Lawn, "Strength and Fatigue Properties of Optical Glass Fibers Containing Microindentation Flaws", *J. Am. Ceram. Soc.*, **68**(11), 563-569 (1985).
17. D.J. Wissuchek, "Effect of refractory particles on the strength of optical fibers", *Mat. Res. Soc. Symp. Proc.*, 531, 187-192 (1998).
18. M. Muraoka, H. Abe, "Subcritical crack growth in silica optical fibers in a wide range of crack velocities," *J. Amer. Ceram. Soc.*, **79**(1), 51-57 (1996).
19. V.A. Bogatyrev, M.M. Bubnov, E.M. Dianov, S.D. Romyantzev, S.L. Semjonov, "Mechanical reliability of polymer-coated and hermetically coated optical fibers based on proof testing," *Opt. Eng.*, **30**(6), 690-699 (1991).